Intermediate Nonlinear Regimes of Line-tied g Mode and Ballooning Instability

P. Zhu 1), C. C. Hegna 1), C. R. Sovinec 1), A. Bhattacharjee 2), K. Germaschewski 2)
1) University of Wisconsin-Madison, Madison, WI 53706, USA
2) University of New Hampshire, Durham, NH 03824, USA

Abstract A theoretical framework has been developed to describe the nonlinear regimes of line-tied g modes in slab geometry and ballooning instabilities in toroidal configurations. This work is motivated by the correlation of edge localized mode (ELM) activity in H-mode plasmas with ideal MHD peeling-ballooning instability. Recent experimental observation and numerical simulations demonstrate a persistence of ballooning-like filamentary structures well into the nonlinear stage. Our theory is based on an expansion using two small scale lengths, which are the mode displacement across magnetic flux surface and the mode width in the most rapidly varying direction, both normalized by the equilibrium scale length. When the mode displacement across magnetic flux surface is much less than the mode width in the most rapidly varying direction, the mode is in the linear regime. When the mode displacement grows to the order of the mode width in the rapidly varying direction, the plasma remains incompressible to lowest order, and the Cowley-Artun regime is obtained. The detonation regime, where the nonlinear growth of the mode could be finite-time singular, is accessible when the system is sufficiently close to marginal stability. At higher levels of nonlinearity, the system evolves to the intermediate nonlinear regime, when the mode displacement across magnetic flux surface becomes comparable of the mode width in the same direction. During this phase, the nonlinear growth of the mode in parallel and perpendicular directions are coupled, and sound wave physics contributes to nonlinear stabilization. The governing equations for the line-tied g mode and the ballooning instability in the intermediate nonlinear regime have been derived. A remarkable feature of the nonlinear equations is that solutions of the associated local linear mode equations continue to be valid solutions into the intermediate nonlinear regime. This property has been confirmed in direct ideal MHD simulations of both the line-tied g mode in a shearless slab and the ballooning instability in a tokamak, and may help explain the persistence of the filamentary ELM structures observed in experiments well into the nonlinear growth phase.

1 Introduction

Filamentary structures and their localization in the unfavorable curvature region of the tokamak edge have been routinely observed during periods of edge localized modes (ELMs) in recent Mega Amp Spherical Tokamak (MAST) experiments [1, 2] and extended magnetohydrodynamic (MHD) simulations [3, 4]. This suggests that the ballooning instability properties of the pedestal region continue to play a dominant role in determining the nonlinear temporal and spatial structures of ELMs. Thus it may be possible to understand the dynamics of the ELM filaments in terms of the nonlinear properties of the ballooning instability. In this work, we develop an ideal MHD theory for the nonlinear evolution of the line-tied g mode in a shearless slab geometry and the ballooning instability in general

toroidal magnetic configurations. We also compare the prediction from theory with our direct MHD simulations of both modes.

For simplicity, in this introduction we use the term "ballooning instability" to refer to both the line-tied g mode in a shearless slab geometry and the ballooning mode in toroidal configurations. This is because both modes share similar linear and nonlinear dynamics despite the very different associated geometry [5, 6]. Due to its simpler geometry, the line-tied g mode has been studied as a prototype for the more geometrically complicated ballooning instability [7, 8, 9, 10, 11].

Different phases of ELMs may relate to different linear and nonlinear regimes of ballooning instability. To describe the different nonlinear phases, we introduce two small parameters given by

$$n^{-1} = \frac{k_\parallel}{k_\perp} \ll 1, \qquad \varepsilon = \frac{|\boldsymbol{\xi}|}{L_{\rm eq}} \ll 1. \tag{1}$$

Here, $k_\parallel$ and $k_\perp$ are the dominant wavenumbers of the perturbation parallel to and perpendicular to the equilibrium magnetic field lines, respectively; $\boldsymbol{\xi}$ is the ideal MHD plasma displacement produced by instability, and $L_{\rm eq}$ is the equilibrium scale length (which is used as the normalization length later so that $L_{\rm eq} = 1$).

The linear structure and growth rates of ballooning instabilities can be determined using an asymptotic expansion of the linearized ideal MHD equation in terms of n^{-1} [12, 13, 14]. The mode structure in the fastest varying direction perpendicular to the field line is given by n^{-1}, which is the scale of the dominant wavelength. At lowest order in n^{-1}, the ballooning mode is described by two coupled one-dimensional ordinary differential equations along each field line, which together with proper boundary conditions, determines the local eigenfrequency or local growth rate as well as the local mode structure along the equilibrium magnetic field as a function of magnetic flux surface, field line, and radial wavenumber. At higher order in n^{-1}, a global eigenmode equation, the envelope equation, which uses information from the local mode calculations, governs the global growth rate and mode structure across magnetic surfaces. In axisymmetric equilibria, the global growth rate is given by the most unstable value of the local growth rate with stabilizing corrections of order n^{-1}. As shown earlier [7, 15, 16, 10, 11] and in this work, the properties of linear ballooning instability are crucial to the construction and understanding of the theory of nonlinear ballooning instability.

The perturbation amplitude of the nonlinear ballooning mode, measured by ε ($\sim |\boldsymbol{\xi}|$), can be compared to the characteristic spatial scales of its linear mode structure. In the early nonlinear regime, the filament scale $|\boldsymbol{\xi}|$ across the magnetic flux surface is comparable to the mode width λ_α in the most rapidly oscillating direction, $|\boldsymbol{\xi}| \sim \lambda_\alpha \sim n^{-1}$ [7, 15, 16]. In this regime, nonlinear convection $|\boldsymbol{\xi}|$ across the flux surface is small relative to the mode width λ_Ψ in that direction, and nonlinearities modify the radial envelope equation describing mode evolution across the magnetic surface. Here Ψ and α are the flux and field line labels, respectively, which are later used to define the equilibrium magnetic field in Eq. (4). As the mode continues to grow, it enters the intermediate nonlinear regime, in which $|\boldsymbol{\xi}| \sim \lambda_\Psi \sim n^{-1/2}$; the plasma displacement across magnetic flux surface becomes of the same order as the mode width in the same direction [10, 11]. In this regime, effects due to convection and compression are no longer small. Nonlinearities due to convection and compression, together with nonlinear line-bending forces, directly modify the "local"

mode evolution along the magnetic field line. In the late nonlinear regime, the ballooning filament growth may exceed the scale of the pedestal width and result in the collapse of the pedestal. Eventually, these ballooning filaments could detach from edge plasma and propagate into the scrape-off-layer region, as indicated from recent experiment [2]. In this work, we consider the physics of the intermediate nonlinear phase and leave discussion of the late nonlinear regime for subsequent work.

It is conceivable that the linear to early nonlinear regime of the ballooning instability of the pedestal may correspond to the precursor phase of ELMs since the onset of the ELMs have been consistently correlated to the breaching of the linear stability boundary of the peeling-ballooning modes [17, 18]. Earlier theory attempted to explain the collapse onset phase of ELMs by invoking a finite time-like singularity associated with the early nonlinear ballooning instability of a marginally unstable configuration ("Cowley-Artun" regime) [7, 15, 16]. Such a scenario, however, has yet to be confirmed by direct MHD simulations, probably due to the rather limited range of validity for that regime. In contrast, there is a good agreement between the solutions of the intermediate nonlinear regime equations and results from direct MHD simulations for both the case of a line-tied g-mode [11] and the ballooning instability of a tokamak [6] (Sec. 3). It is likely that the intermediate nonlinear regime may better characterize the transition from the precursor phase to the collapse onset of an ELM. This regime could become particularly relevant for a transport barrier as the width of that barrier (or pedestal) region approaches the mode width of the dominant ballooning mode.

In this work, an ideal MHD model is employed. However, the effects outside of ideal MHD model could also play an important role in the nonlinear phase. In particular, it is noted that FLR (finite Larmor radius) and two-fluid effects can significantly alter the ELM filament dynamics, as indicated by the recent MHD simulations with the NIMROD code [3, 4]. Whereas the FLR and two-fluid effects are well known to stabilize the linear ballooning modes with sufficiently high-n mode numbers, their exact roles in the nonlinear ballooning and ELM filament dynamics remain unclear. Earlier nonlinear theory of the ballooning-like, line-tied g mode considered the linear contribution from the ion diamagnetic drift [8]. Their analysis suggests that the linear stabilization due to FLR effects do not seem to alter the nonlinear growth rate. Similar findings were reported in recent two-fluid MHD simulations of ELMs, where the FLR effects were found to alter nonlinear filament and flow patterns, but did not significantly change the mode growth [19]. These two-fluid MHD simulations of ballooning filament are reminiscent of previous two-fluid simulations of magnetic Rayleigh-Taylor instability or g-mode, where the physics is expected to be similar [20, 21, 22]. Before embarking on a detailed nonlinear study of a more sophisticated two-fluid model, a systematic study of the ideal MHD model is undertaken in the present study.

In the rest of the paper, we first lay out the general equations of the intermediate nonlinear regime for both the line-tied g mode and the ballooning instability. We then review the comparisons between the theory and direct MHD simulations of the line-tied g mode and the ballooning instability, respectively. Finally we conclude with a summary and discussion.

2 Theory

The nonlinear theory of ballooning mode can be conveniently developed in the Lagrangian formulation of the ideal MHD model [23]

$$\frac{\rho_0}{J}\nabla_0\mathbf{r}\cdot\frac{\partial^2\boldsymbol{\xi}}{\partial t^2}=-\nabla_0\left[\frac{p_0}{J^\gamma}+\frac{(\mathbf{B}_0\cdot\nabla_0\mathbf{r})^2}{2J^2}\right]+\nabla_0\mathbf{r}\cdot\left[\frac{\mathbf{B}_0}{J}\cdot\nabla_0\left(\frac{\mathbf{B}_0}{J}\cdot\nabla_0\mathbf{r}\right)\right]+\frac{\rho_0}{J}\nabla_0\mathbf{r}\cdot\mathbf{g} \quad (2)$$

where

$$\mathbf{r}(\mathbf{r}_0,t)=\mathbf{r}_0+\boldsymbol{\xi}(\mathbf{r}_0,t),\quad \nabla_0=\frac{\partial}{\partial\mathbf{r}_0},\quad J(\mathbf{r}_0,t)=|\nabla_0\mathbf{r}|. \quad (3)$$

Here, $\mathbf{r}_0$ denotes the initial location of each plasma element in the equilibrium, $\boldsymbol{\xi}$ is the plasma displacement from the initial location, and $J(\mathbf{r}_0,t)$ is the Jacobian for the Lagrangian transformation from $\mathbf{r}_0$ to $\mathbf{r}(\mathbf{r}_0,t)$; ρ_0, p_0, and $\mathbf{B}_0$ are the equilibrium mass density, pressure, and magnetic field, respectively. We consider a general magnetic configuration that can be described by

$$\mathbf{B}_0=\nabla_0\Psi_0\times\nabla_0\alpha_0 \quad (4)$$

in a nonorthogonal Clebsch coordinate system (Ψ_0,α_0,l_0), where Ψ_0 is the magnetic flux label, α_0 the field line label, and l_0 the measure of field line length. The corresponding coordinate Jacobian is given by $(\nabla_0\Psi_0\times\nabla_0\alpha_0\cdot\nabla_0 l_0)^{-1}=|\mathbf{B}_0|^{-1}$.

The intermediate nonlinear regime is defined by the ordering $\varepsilon\sim\mathcal{O}(n^{-1/2})$ [10, 11]. In this regime the plasma displacement $\boldsymbol{\xi}$ and the Lagrangian Jacobian J are expanded as a single series in $n^{-1/2}$

$$\boldsymbol{\xi}(\sqrt{n}\Psi_0,n\alpha_0,l_0,t) = \sum_{j=1}^{\infty}n^{-\frac{j}{2}}\left(\mathbf{e}_\Psi\xi^\Psi_{\frac{j}{2}}+\frac{\mathbf{e}_\alpha}{\sqrt{n}}\xi^\alpha_{\frac{j+1}{2}}+\mathbf{b}\xi^l_{\frac{j}{2}}\right), \quad (5)$$

$$J(\sqrt{n}\Psi_0,n\alpha_0,l_0,t) = 1+J_0+\sum_{j=1}^{\infty}n^{-\frac{j}{2}}J_{\frac{j}{2}}. \quad (6)$$

where $\mathbf{e}_\Psi=B_0^{-1}\nabla_0\alpha_0\times\nabla_0 l_0$, $\mathbf{e}_\alpha=B_0^{-1}\nabla_0 l_0\times\nabla_0\Psi_0$, $\mathbf{e}_l=B_0^{-1}\mathbf{B}_0=\mathbf{b}$, and $B_0=|\mathbf{B}_0|$. Here and subsequently we drop the subscript "0" in the equilibrium MHD fields ρ_0, p_0, and $\mathbf{B}_0$ for convenience. The plasma displacement $\boldsymbol{\xi}$ and the Lagrangian Jacobian J are functions of the normalized coordinates (Ψ,α,l), where $\Psi=\sqrt{n}\Psi_0$, $\alpha=n\alpha_0$, $l=l_0$.

For convenience, a new set of basis vectors are introduced [15]

$$\mathbf{e}_\perp=\mathbf{e}_\Psi\cdot(\mathbf{I}-\mathbf{bb})=\frac{\nabla_0\alpha_0\times\mathbf{B}}{B^2},\quad \mathbf{e}_\wedge=\mathbf{e}_\alpha\cdot(\mathbf{I}-\mathbf{bb})=\frac{\mathbf{B}\times\nabla_0\Psi_0}{B^2} \quad (7)$$

so that

$$\boldsymbol{\xi}=\mathbf{e}_\perp\xi^\Psi+\mathbf{e}_\wedge\xi^\alpha+\mathbf{B}\xi^\parallel. \quad (8)$$

At the third order of expansion, the governing equations for the intermediate nonlinear regime ($\varepsilon\sim n^{-1/2}$) can be obtained in the following compact form [5]

$$\left[\Psi+\xi^\Psi_{\frac{1}{2}},\rho|\mathbf{e}_\perp|^2\partial_t^2\xi^\Psi_{\frac{1}{2}}-\mathcal{L}_\perp(\xi^\Psi_{\frac{1}{2}},\xi^\parallel_{\frac{1}{2}})\right]=0, \quad (9)$$

$$\rho B^2\partial_t^2\xi^\parallel_{\frac{1}{2}}-\mathcal{L}_\parallel(\xi^\Psi_{\frac{1}{2}},\xi^\parallel_{\frac{1}{2}})=0. \quad (10)$$

where $\partial_t = (\partial/\partial t)_{\mathbf{r}_0}$, $[A, B] \equiv \partial_\Psi A \partial_\alpha B - \partial_\alpha A \partial_\Psi B$, $\mathcal{L}_\perp$ ($\mathcal{L}_\parallel$) is the perpendicular (parallel) component of the local linear ballooning and g mode operator [15, 5]. In general, equations (9) and (10) require numerical solution. However, the structure of these two equations indicates that the solution satisfies the following general form

$$\rho|\mathbf{e}_\perp|^2 \partial_t^2 \xi^\Psi_{\frac{1}{2}} = \mathcal{L}_\perp(\xi^\Psi_{\frac{1}{2}}, \xi^\parallel_{\frac{1}{2}}) + N(\Psi + \xi^\Psi_{\frac{1}{2}}, l, t), \tag{11}$$

$$\rho B^2 \partial_t^2 \xi^\parallel_{\frac{1}{2}} = \mathcal{L}_\parallel(\xi^\Psi_{\frac{1}{2}}, \xi^\parallel_{\frac{1}{2}}) \tag{12}$$

where $N(\widetilde{\Psi}, l, t)$ is a function of the distorted flux function

$$\widetilde{\Psi} = \Psi + \xi^\Psi_{\frac{1}{2}}, \tag{13}$$

in addition to the field line coordinate l and time. A particular choice is

$$N(\widetilde{\Psi}, l, t) = 0, \tag{14}$$

which implies that the solutions of the linear local ballooning mode equations will continue to be the solution of the nonlinear ballooning equations (9) and (10). The nonlinearities in equations (9) and (10) would vanish for any nonlinear solution that assumes the linear ballooning mode structure in the Lagrangian coordinates. As a consequence, globally the mode will grow exponentially at the growth rate of the corresponding linear phase even in the intermediate nonlinear stage. As shown in next section, recent direct MHD simulations have confirmed this theory prediction.

3 Comparisons with Direct MHD Simulations

Direct ideal MHD simulations of the line-tied g mode have been performed for a shearless slab configuration (Fig. 1) using the BIC code [9]. A Cartesian coordinate system is adopted, with $\hat{\mathbf{x}}$, $\hat{\mathbf{y}}$, and $\hat{\mathbf{z}}$ being the basis vectors. The equilibrium field $\mathbf{B}_0$ is tied to two ends in the z-direction; the gradients of the equilibrium density ρ_0 and pressure p_0 are in the direction of $\hat{\mathbf{x}}$ perpendicular to field lines, and the gravity $\mathbf{g}$ is in the direction of $-\hat{\mathbf{x}}$. The intermediate nonlinear equations (9) and (10) are solved numerically for the line-tied g mode with the same initial and boundary conditions as those used in the corresponding direct MHD simulation [11]. The growth of the maximum of the x-component of the flow ($u_x = \partial_t \xi_x$) obtained from both the numerical solution and the MHD simulation are plotted in Fig. 1. The prediction from the asymptotic theory agrees well with the result from the simulation throughout the linear and the intermediate nonlinear phases. In particular, both the numerical solution and the simulation result demonstrate a nearly exponential mode growth in the intermediate nonlinear phase, consistent with our analytic theory.

The analytic solution of the nonlinear ballooning equations has also been verified in recent simulations of nonlinear ballooning instability in a tokamak [6] using the NIRMOD code [24]. The simulation starts with a small perturbation to a simple tokamak equilibrium generated with the ESC solver [25] (Fig. 2). The initial perturbation is dominated by a $n = 15$ component (where n is the toroidal mode number). In the NIMROD simulation, we advance the plasma displacement as an extra field in Eulerian coordinates using

$$\partial_t \boldsymbol{\xi}(\mathbf{r}, t) + \mathbf{u}(\mathbf{r}, t) \cdot \nabla \boldsymbol{\xi}(\mathbf{r}, t) = \mathbf{u}(\mathbf{r}, t) \tag{15}$$

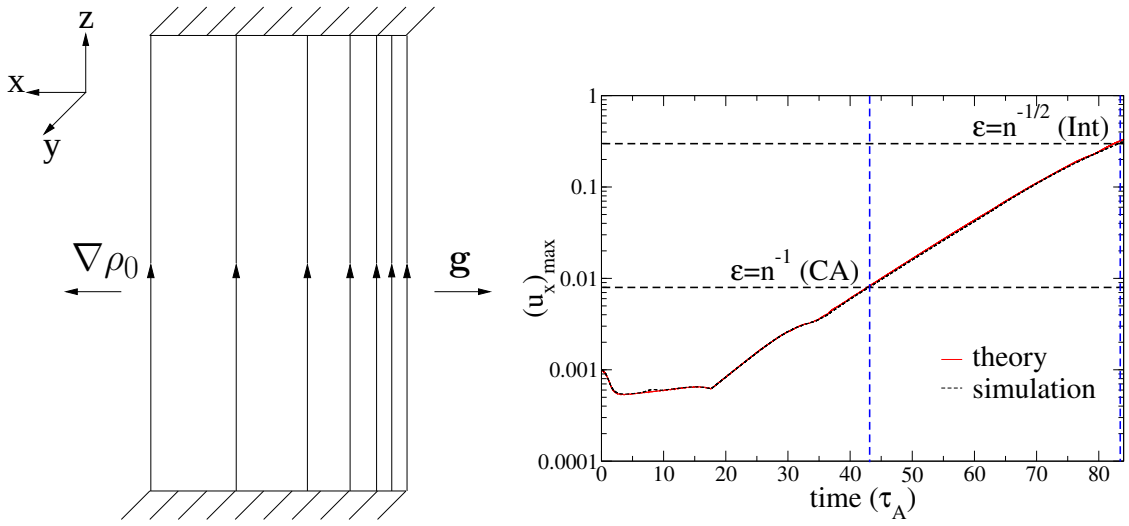

Figure 1: Left: A shearless slab configuration of line-tied flux tubes; Right: Growth of the maximum of flow in the x direction obtained from theory (solid red line) and simulation (broken black line). The maximum of the initial flow is $u_{x0} = 10^{-3}$. The two horizontal (vertical) broken lines represent the Cowley-Artun ("CA") regime and the intermediate regime (denoted as "Int") in mode magnitude (in time) respectively.

where $\mathbf{u}(\mathbf{r}, t)$ is the velocity field, $\partial_t = (\partial/\partial t)_{\mathbf{r}}$, and $\nabla = \partial/\partial\mathbf{r}$. We then calculate the Lagrangian divergence $\nabla_0 \cdot \boldsymbol{\xi}$ from the Eulerian tensor $\nabla\boldsymbol{\xi}$ using the identity

$$\nabla_0 \cdot \boldsymbol{\xi} = \mathrm{Tr}(\nabla_0\boldsymbol{\xi}) = \mathrm{Tr}[(\mathbf{I} - \nabla\boldsymbol{\xi})^{-1} \cdot \nabla\boldsymbol{\xi}]. \tag{16}$$

Both the maximum plasma displacement $|\boldsymbol{\xi}|_{\max}$ and the maximum Lagrangian divergence $(\nabla_0 \cdot \boldsymbol{\xi})_{\max}$ of the entire simulation domain evolve at the same linear growth rate during the phase $5 \lesssim t <\lesssim 20$. As the Lagrangian divergence $(\nabla_0 \cdot \boldsymbol{\xi})_{\max}$ becomes of order unity, its growth starts to deviate from the linear exponential growth. This is the indication that the perturbation has evolved into the intermediate nonlinear phase, which is characterized by the ordering

$$\boldsymbol{\xi} \cdot \nabla_0 \sim \nabla_0 \cdot \boldsymbol{\xi} \sim \lambda_\Psi^{-1}\xi^\Psi + \lambda_\alpha^{-1}\xi^\alpha \sim 1. \tag{17}$$

However, the maximum plasma displacement itself continues to grow exponentially well into the intermediate nonlinear phase, as demonstrated in Fig. 2, and as predicted by the special solution of the analytic theory (Sec. 2) [5]. The sudden enhanced growth of the Lagrangian divergence $\nabla_0 \cdot \boldsymbol{\xi}$ above the intermediate nonlinear regime may reflect the fact that the matrix $(\mathbf{I} - \nabla\boldsymbol{\xi})$ could become nearly singular during the nonlinear phase, even though the Eulerian divergence $\nabla \cdot \boldsymbol{\xi}$ remains regular. For the case shown in Fig. 2, the tokamak minor radius is $a = 1$, and the pressure pedestal width is $L_p \sim 0.1$. As the mode transverses the intermediate nonlinear phase, the maximum plasma displacement $|\boldsymbol{\xi}|_{\max}$ approaches the pedestal scale length L_p.

4 Summary and Discussion

An ideal MHD theory for the line-tied g mode and the ballooning instability in the intermediate nonlinear regime has been developed in general toroidal magnetic configurations.

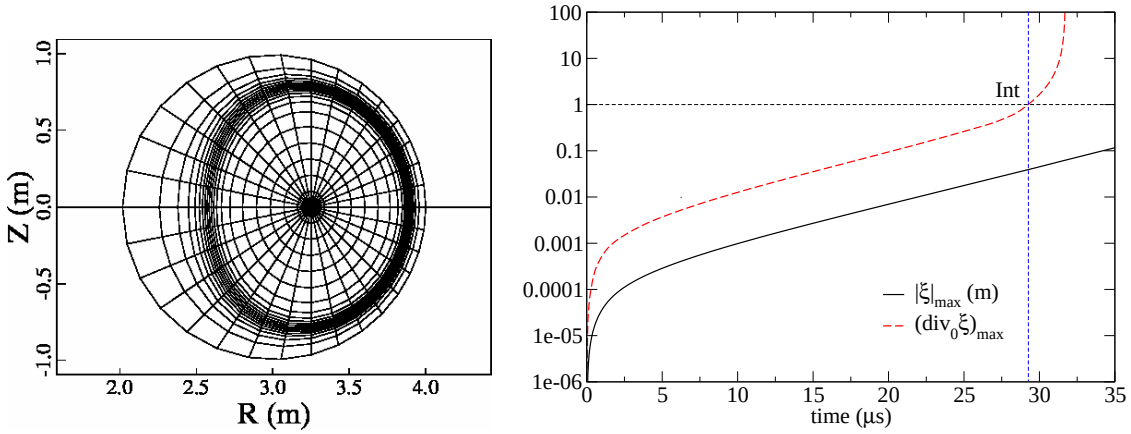

Figure 2: Left: The finite element mesh based on a tokamak equilibrium generated using the ESC solver; Right: Growth of the maximum amplitude of plasma displacement $|\boldsymbol{\xi}|_{\max}$ (black solid line) and growth of the maximum Lagrangian divergence $(\nabla_0 \cdot \boldsymbol{\xi})_{\max}$ (red broken line) calculated from a NIMROD simulation. The unit of the plasma displacement $\boldsymbol{\xi}$ is meter. The horizontal and vertical broken lines mark the intermediate nonlinear regime as determined by $\nabla_0 \cdot \boldsymbol{\xi} \sim 1$ (denoted as "Int").

In this nonlinear regime, there are three major nonlinear effects that are involved in the development of a ballooning filament due to radial convection, line bending, and magnetosonic coupling.

A remarkable property of the intermediate nonlinear regime is that, solutions of the associated linear local ballooning mode equations continue to be solutions of the intermediate nonlinear ballooning equations [Eqs. (9) and (10)]. This implies that a perturbation that evolves from a linear line-tied g mode or ballooning instability will continue to grow exponentially at the same growth rate globally, and maintain its filamentary mode structure of the corresponding linear phase in the intermediate nonlinear stage in the Lagrangian coordinates. This may explain why in experiments the nonlinear ELM filament strongly resembles the structure of a linear ballooning filament, and linear analyses have often been able to match and predict the observations in ELM experiments [18, 26]. The theory prediction is consistent with numerical analysis and simulations of the line-tied g mode [9, 11], and is also verified in recent direct MHD simulations of tokamak ballooning instability [6]. This agreement between theory and simulations is a step toward understanding the precursor and onset phases of ELMs.

Our analytical model focuses on the nonlinear growth of the ballooning filament in the ideal MHD regime. The adoption of the ideal MHD model by no means implies the insignificance of other nonideal MHD effects (two-fluid physics, resistivity, FLR, etc.) on ballooning filament dynamics. Rather, this approach allows the systematic isolation, identification, and inclusion of the dominant nonlinear mechanisms in each relevant MHD regime. Our study in this work is only the first necessary step towards the construction of a more relevant two-fluid MHD model for the dynamics of nonlinear ballooning and ELM filaments. It is our plan to introduce the FLR and two-fluid effects to our model for nonlinear ballooning filament in the near future.

5 Acknowledgments

This research is supported by U.S. Department of Energy under Grant No. DE-FG02-86ER53218. The authors are grateful for discussions with J. D. Callen and S. C. Cowley.

References

[1] Kirk, A., Koch, B., Scannell, R., Wilson, H. R., Counsell, G., Dowling, J., Herrmann, A., Martin, R., Walsh, M., and the MAST team, "Evolution of filament structures during edge-localized modes in the MAST tokamak," *Phys. Rev. Lett.* **96** (2006) 185001.

[2] Kirk, A., Counsell, G. F., Cunningham, G., Dowling, J., Dunstan, M., Meyer, H., M.Price, S.Saarelma, R.Scannell, M.Walsh, Wilson, H. R., and the MAST team, "Evolution of the pedestal on MAST and the implications for ELM power loadings," *Plasma Phys. Control. Fusion* **49** (2007) 1259.

[3] Sovinec, C. R., Schnack, D. D., Pankin, A. Y., Brennan, D. P., Tian, H., Barnes, D. C., Kruger, S. E., Held, E. D., Kim, C. C., Li, X. S., Kaushik, D. K., Jardin, S. C., and the NIMROD Team, "Nonlinear extended magnetohydrodynamics simulation using high-order finite elements," *J. Phys.: Conf. Ser.* **16** (2005) 25.

[4] Sovinec, C. R., Barnes, D. C., Bayliss, R. A., Brennan, D. P., Held, E. D., Kruger, S. E., Pankin, A. Y., Schnack, D. D., and the NIMROD Team, "Two-fluid studies of edge relaxation events in tokamaks," *J. Phys.: Conf. Ser.* **78** (2007) 012070.

[5] Zhu, P. and Hegna, C. C., "Ballooning filament growth in the intermediate nonlinear regime," *Phys. Plasmas* **15** (2008) 092306.

[6] Zhu, P., Hegna, C. C., and Sovinec, C. R., "Nonlinear ballooning filament: Structure and growth," In preparation (2008).

[7] Cowley, S. C. and Artun, M., "Explosive instabilities and detonation in magnetohydrodynamics," *Phys. Rep.* **283** (1997) 185.

[8] Fong, B. H., Cowley, S. C., and Hurricane, O. A., "Metastability in magnetically confined plasmas," *Phys. Rev. Lett.* **82** (1999) 4651.

[9] Zhu, P., Bhattacharjee, A., and Germaschewski, K., "Intermediate nonlinear evolution of the Parker instability: Formation of convection-induced discontinuities and absence of finite-time singularities," *Phys. Rev. Lett.* **96** (2006) 065001.

[10] Zhu, P., Hegna, C. C., and Sovinec, C. R., "Nonlinear growth of a line-tied g mode near marginal stability," *Phys. Plasmas* **13** (2006) 102307.

[11] Zhu, P., Hegna, C. C., Sovinec, C. R., Bhattacharjee, A., and Germaschewski, K., "Intermediate nonlinear regime of a line-tied g mode," *Phys. Plasmas* **14** (2007) 055903.

[12] Connor, J. W., Hastie, R. J., and Taylor, J. B., "Shear, periodicity, and plasma ballooning modes," *Phys. Rev. Lett.* **40** (1978) 396.

[13] Connor, J. W., Hastie, R. J., and Taylor, J. B., "High mode number stability of an axisymmetric toroidal plasma," *Proc. R. Soc. Lond. A.* **365** (1979) 1.

[14] Dewar, R. L. and Glasser, A. H., "Ballooning mode spectrum in general toroidal systems," *Phys. Fluids* **26** (1983) 3038.

[15] Hurricane, O. A., Fong, B. H., and Cowley, S. C., "Nonlinear magnetohydrodynamic detonation: Part I," *Phys. Plasmas* **4** (1997) 3565.

[16] Wilson, H. R. and Cowley, S. C., "Theory for explosive ideal magnetohydrodynamic instabilities in plasmas," *Phys. Rev. Lett.* **92** (2004) 175006.

[17] Hegna, C. C., Connor, J. W., Hastie, R. J., and Wilson, H. R., "Toroidal coupling of ideal magnetohydrodynamic instabilities in tokamak plasmas," *Phys. Plasmas* **3** (1996) 584.

[18] Snyder, P. B., Wilson, H. R., Ferron, J. R., Lao, L. L., Leonard, A. W., Osborne, T. H., Turnbull, A. D., Mossessian, D., Murakami, M., and Xu, X. Q., "Edge localized modes and the pedestal: A model based on coupled peeling-ballooning modes," *Phys. Plasmas* **9** (2002) 2037.

[19] Khan, R., Mizuguchi, N., Nakajima, N., and Hayashi, T., "Dynamics of the ballooning mode and the relation to edge-localized modes in a spherical tokamak," *Phys. Plasmas* **14** (2007) 062302.

[20] Huba, J. D., "Finite Larmor radius magnetohydrodynamics of the Rayleigh–Taylor instability," *Phys. Plasmas* **3** (1996) 2523.

[21] Huba, J. D. and Winske, D., "Rayleigh–Taylor instability: Comparison of hybrid and nonideal magnetohydrodynamic simulations," *Phys. Plasmas* **5** (1998) 2305.

[22] Zhu, P., Sovinec, C. R., and Hegna, C. C., "Blob formation in late nonlinear stage of a g mode: Ideal and two-fluid MHD models," NIMROD Team Meeting, Madison, WI, July 16-18, 2007.

[23] Pfirsch, D. and Sudan, R. N., "Nonlinear ideal magnetohydrodynamics instabilities," *Phys. Fluids B* **5** (1993) 2052.

[24] Sovinec, C., Glasser, A., Barnes, D., Gianakon, T., Nebel, R., Kruger, S., Schnack, D., Plimpton, S., Tarditi, A., Chu, M., and the NIMROD Team, "Nonlinear magnetohydrodynamics with high-order finite elements," *J. Comput.Phys.* **195** (2004) 355.

[25] Zakharov, L. E. and Pletzer, A., "Theory of perturbed equilibria for solving the Grad–Shafranov equation," *Phys. Plasmas* **6** (1999) 4693.

[26] Snyder, P. B., Wilson, H. R., and Xu, X. Q., "Progress in the peeling-ballooning model of edge localized modes: Numerical studies of nonlinear dynamics," *Phys. Plasmas* **12** (2005) 056115.